Observations of Planetary Boundary Layer Ozone Concentrations Using Unmanned Aircraft Systems

CHALITA THOMPSON*

National Weather Center Research Experiences for Undergraduates Program
Norman, Oklahoma

ELIZABETH A. PILLAR-LITTLE AND TYLER M. BELL

School of Meteorology, University of Oklahoma
and Center for Autonomous Sensing and Sampling, University of Oklahoma
Norman, Oklahoma

BRIAN R. GREENE

School of Meteorology, University of Oklahoma
Center for Autonomous Sensing and Sampling, University of Oklahoma
and Advanced Radar Research Center, University of Oklahoma
Norman, Oklahoma

ABSTRACT

Ozone is found in abundance in the stratosphere but is also found in smaller, yet more harmful quantities, in the troposphere. This tropospheric ozone can cause public health concerns as well as agricultural damage. The focus of this research project is on the production of ozone in the planetary boundary layer during the day and how it is affected by the nocturnal low-level jet at night. Several methods are presently used to measure ozone concentration in the atmosphere. Ozonesondes can build a vertical profile of the atmosphere but are limited in number while ground stations monitor ozone concentration at the surface. Satellites are also used to measure ozone but do not provide details regarding concentration gradients in the planetary boundary layer. The use of unmanned aircraft systems can allow researchers to build a vertical profile of the planetary boundary layer. The unmanned aircraft system (UAS) is customizable and versatile which gives flexibility to researchers allowing them measure ozone concentrations as well as other atmospheric parameters such as trace gases, temperature, humidity, and aerosols.

1. Introduction and Background

Ozone is a natural greenhouse gas and is a key component of the atmosphere. The stratospheric ozone layer shields the planet by absorbing harmful UV-B radiation from the Sun. However, tropospheric ozone is considered a pollutant because it can negatively impact public health and the biosphere. Exposure to elevated concentrations of ozone damages and irritates tissues of the lungs, nose, throat, leading to increased occurrence of asthma, sore throat, bronchitis, infections, chronic obstructive pulmonary disease, and other respiratory conditions. Small children, the ill, and elderly members of the population are more susceptible even at lower concentrations (Environmental Protection Agency 2019b). Tropospheric ozone has a negative effect on agriculture as well as health. Ozone causes crop yields to decline by entering the plant through the stomata during its normal gas exchange. The water in the plants cells begin to disassociate the ozone molecules then enter into the cells. The resulting structural damage decreases the cell membrane permeability which leads to an increase of CO_2 inside the leaves, causing the plant to die. (Felzer et al. 2007).

Tropospheric ozone is formed as a secondary pollutant when volatile organic compounds (VOC), such as benzene, isoprene, and methane, react with nitric oxide or nitrogen dioxide (NO_x), O_2, and sunlight to form secondary pollutants (Eq. 1).

$$\text{VOCs} + \text{NO}_x + \text{O}_2 + \text{sunlight} \Rightarrow \text{O}_3,\ \text{HNO}_3,\ \text{oxidized VOCs} \quad (1)$$

*Corresponding author address: Chalita Thompson, University of Central Oklahoma, 120 David L. Boren Blvd., Ste. 2500, Norman, OK 73072
E-mail: cnoble1@uco.edu

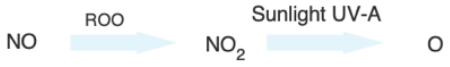

FIG. 1. Cycle of free radical oxygen production. NO reacting with peroxy to form NO_2 , then NO_2 reacting with sunlight to form O•free radical. Adapted from Baird and Cann (2012).

Primary pollutants are pollutants that are released directly into the atmosphere such as sulfur dioxide, nitric oxide, and VOCs. They are primarily released from manufacturing and vehicle emissions. Secondary pollutants are formed when one primary pollutant reacts with another in the presence of sunlight and oxygen to form pollutants such as NO_2, nitric acid, and sulfuric acid (Manahan 2010). Equation 2 shows the reaction of NO_2 in the presence of sunlight (UV-A). NO_2 will decompose to O and NO in the process known as photolysis. The oxygen atoms then react with molecular oxygen (O_2) in the atmosphere to form O_3 (Eq. 3).

$$NO_2 + \text{UV-A} \Rightarrow NO + O \tag{2}$$

$$O + O_2 \Rightarrow O_3 \tag{3}$$

As shown in Figure 1, Organic peroxy free radicals (ROO•) can react with NO to form more NO_2, which keeps the process repeating. This reaction is significantly more favorable during the day as the rate of reaction is increased with the addition of heat and light, leading to increased tropospheric ozone production. Therefore, ozone concentrations typically increase after sunrise, peak in the late afternoon, and begin to decrease at sunset as temperatures decline (Baird and Cann 2012; Zielke 2011). Furthermore, O_3 concentrations in urban areas tend to be higher compared to rural and remote locations since VOC emissions from fossil fuel combustion and manufacturing facilities add to naturally occurring VOCs emitted by the biosphere (Baird and Cann 2012).

Earths ozone concentrations are measured via several methods. State and federal agencies such as the Oklahoma Department of Environmental Quality and Environmental Protection Agency monitor tropospheric ozone at fixed points using ground stations throughout the United States. While a ground station can provide baseline data continuously over time for a specific location, they are spatially limited by their footprint and vertical extent. As observed in Figure 2, the ozone monitoring network also has poor spatial resolution in the Plains and Mountain West regions of the country.

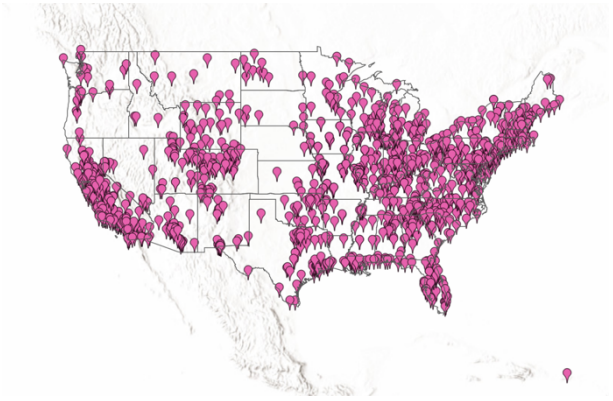

FIG. 2. EPA Map of ozone monitoring ground stations in U.S. Adapted from Environmental Protection Agency (2019a).

FIG. 3. Ozonesonde Vertical profile network. Circles are NOAA launch sites. Stars represent Southern Hemisphere Additional Ozonesonde (SHADOZ), NOAA collaboration sites. Adapted from National Oceanic and Atmospheric Administration (2018).

Ozonesondes operate similarly to radiosondes, except they monitor ozone concentrations instead of typical meteorological parameter. They have the benefit of providing researchers with a vertical profile of the atmosphere due to their ability to sample at higher altitudes than ground stations. Use of ozonesondes furnishes the ability to measure ozone concentrations at higher altitudes, but these are expensive and are only used about every 1-3 weeks. They do not spend much time in the troposphere, but move quickly through the atmosphere sampling a large column of air. There are only a handful of sites worldwide that launch ozonesondes, which makes observation in most heavily populated and urban areas non-existent (Figure 3).

The European Space Agency and NASA use satellites to monitor ozone concentrations. NASA uses the Ozone Monitoring Instrument (OMI) mounted on the Aura satellite to determine ozone concentrations. OMI has the capability to provide ozone concentrations at the top of the troposphere as well as the ability to measure different atmospheric constituents (National Aeronautics and Space Administration 2019). This provides a top down analysis of the ozone concentration above Earths surface. How-

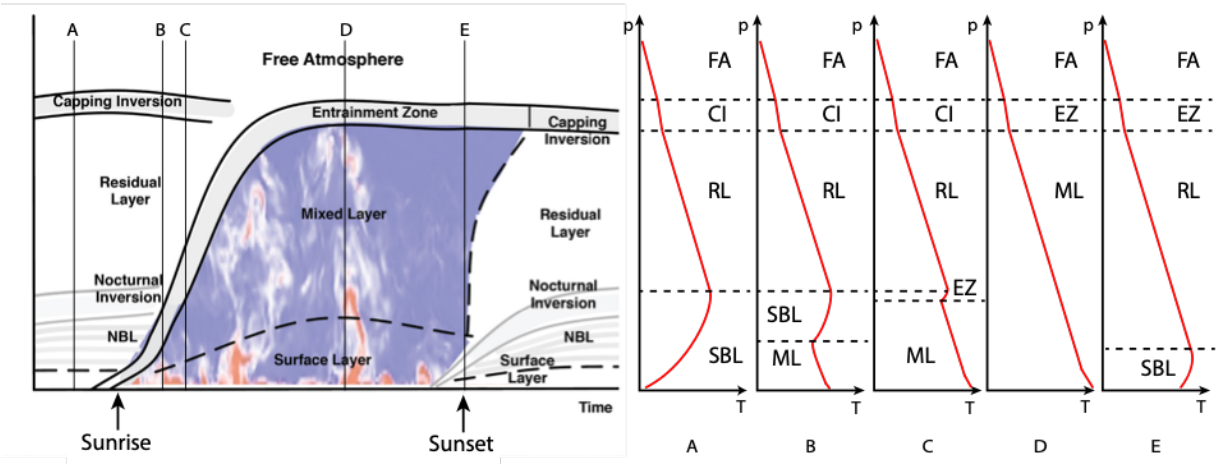

FIG. 4. Diurnal cycle of the vertical structure of the PBL.

ever, this method does not measure ozone exclusively in the planetary boundary layer (PBL). While these methods are effective for their individual applications, these techniques leave significant gaps in the data collected in space and time.

2. Motivation

The planetary boundary layer is the bottom layer of the troposphere. The PBL follows a diurnal cycle in which a mixed layer (ML) of turbulence deepens as the day progresses (Figure 4). This mixed layer is capped by a stable entrainment zone. At sunset the turbulence begins to subside, and the mixed layer transitions into a residual layer. Over the course of the evening, the portion of the residual layer that is closest to the surface becomes a stable boundary layer (SBL) due to radiative cooling from the surface. A strong temperature inversion will often occur here due to the radiative cooling (Stull 1988).

As unmanned aircraft systems (UAS) become more commercially available, there is a greater interest in using these tools to sample the PBL to a far greater extent than towers, radiosondes, and satellites. Harnessing these capabilities requires expertise across several disciplines including chemistry, atmospheric sciences, and electrical, computer, mechanical, and aerospace engineering. Leveraging this new technology, the aim of this project is to gain a better understanding of the vertical and temporal distribution of ozone in the PBL by integrating ozone sensors into a UAS. With careful calibration and deliberate integration, we expect to gain a better understanding of the local and regional variations in ozone concentration and examine how this relates to local air quality, weather conditions, and emissions.

3. Materials and Methods

a. Sensors

This study utilized an Aeroqual SM50 electrochemical ozone sensor. The Aeroqual ozone sensor is an electrochemical sensor that uses heated tungsten trioxide to create an energy potential. When air comes in contact with the WO_3 porous layer, O_3 fills the empty spaces. This leads to a decrease in the charge and an increase in the resistance. When O_3 is not present or is present in decreased amounts, oxygen is expelled from the porous surface which causes the resistance to decrease due to an increase in the charge of the surface (Williams 1999). The resulting change is converted to a voltage differential and then output as a concentration based on a factory calibration.

The ozone sensor requires a 12 V power supply and uses a maximum of 6 W of power when the fan is drawing air into the sensing chamber. The sensor was chosen because it was previously used in the work performed by Zielke (2011). Additionally, it has a high resolution and accuracy in sensing atmospherically relevant concentrations of ozone, on the order of 0–150 ppb, with an accuracy of $\pm$5 ppb. The sensor can operate in a wide range of relative humidities (5–95%) and temperatures (-5–40°C) with minimal impacts to accuracy. The sensor has a response time of 70 s according to the manufacturers specifications. This response time allows the sensor to sample a larger volume of air. The ideal environment for sampling ozone with the SM50 is in calm conditions with smooth airflow.

When first powered on, the sensor must warm up for 3–4 min. The sensor system includes a small fan that draws a fresh air sample over the sensor for 30 s. The fan stops for another 30 s while the data are averaged and transmitted to the data logger.

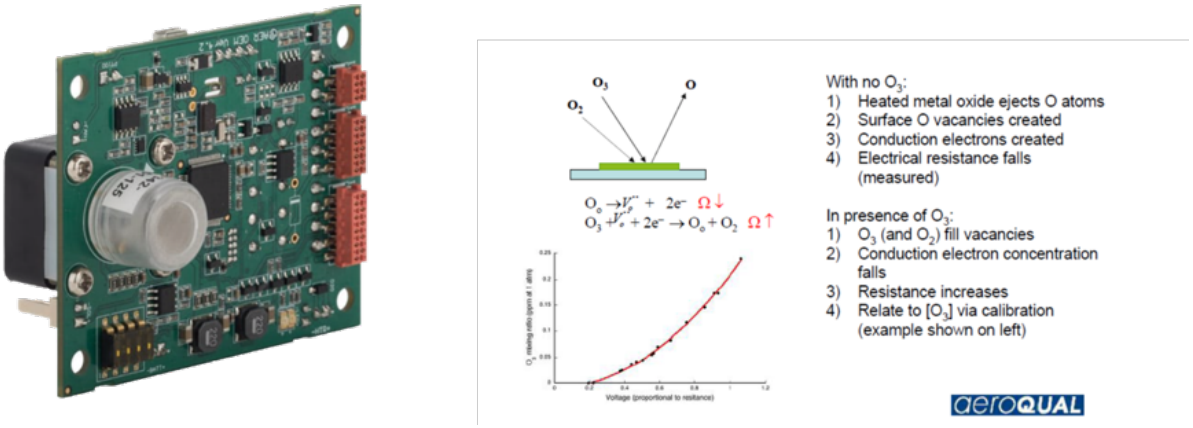

FIG. 5. Aeroqual SM50 ozone sensor (left). Means by which the SM50's heated WO_3 surface collects ozone and outputs a voltage consistent to the ozone concentration (right) (from Aeroqual Ltd., 2019)

b. CopterSonde 3

The UAS utilized to fly the ozone payload was the CopterSonde 3, designed by the Center for Automous Sensing and Sampling (Figure 6). This CopterSonde is the third design iteration of the original rwUAS described in Greene et al. 2018 and is intended for heavier payloads. The Y6-style vehicle frame is comprised of a carbon fiber plate fuselage, carbon fiber tube arms, and carbon fiber curved rectangular rod legs and has six fixed-pitch rotors, with two each mounted at the ends of three arms attached to the main body. The CopterSonde utilizes six carbon fiber 14 in diameter and 4.8 in/rev pitch T-style propellers, each driven by a T-motor U7 700 kV brushless electric motor (Nanchang, China) and a Lumenier 50 A BLHeli32 4-in-1 speed controller (Sarasota, FL, USA).

FIG. 6. Photo of the CopterSonde 3, the rotary-wing Y6 UAS utilized in this study to sample vertical profiles of O_3.

The flight endurance is about 25 min with a payload of 0.5 kg and a total all-up weight of 4.1 kg, and a top flight speed of 22 m s-1.The CopterSonde is equipped with a Pixhawk Cube 2.1 autopilot board (Hex Technology, Sha Tin, Hong Kong), which was used as the main controller for flight stabilization, navigation and operation. This autopilot system is capable of real-time kinematics (RTK) differential GPS (DGPS), which allows for positional accuracy on the order of centimeters. The Pixhawk runs open-source ArduCopter algorithms, which have been customized to add compatibility with the desired atmospheric sensors and allows for collected data to stream to the ground station over telemetry in real time.

With the use of Mission Planner, a flight path can be programmed for uniform and repeatable sampling patterns. A customized, sealed, box was 3-D printed to house the sensor and is mounted to the coptersonde. The box contains two sensors, two diaphragm pumps, and an analog to digital converter (ADC). The ADC is used to translate the voltage output of the SM50 into a digital output that can be recorded by the Pixhawk, which is serving as the datalogger. This allows the data to be streamed live to the ground station via the telemetry link for monitoring as well as saved alongside the flight data.

The use of a rotorcraft for this study is advantageous in that it will allow for atmospheric sampling without the need for a runway or extensive pilot training and it is easier to customize. The Pixhawk 2.1 autopilot board is an open-hardware project that allows for autonomous flight control when combined with the Ardupilot software. With the use of Mission Planner, a flight path can be programmed for uniform and repeatable sampling patterns. A customized, sealed, box was 3-D printed to house the sensor and is mounted to the coptersonde. The box contains two sensors, 2 diaphragm pumps, and an analog to digital converter (ADC). The ADC is used to translate the voltage output of the SM50 into a digital output that can be recorded by the Pixhawk, which is serving as the datalogger. This allows the data to be streamed live to the ground station for monitoring as well as saved alongside the flight data. This setup was chosen to allow the sensor fan to pull in air when it was operating, much as it would in the field.

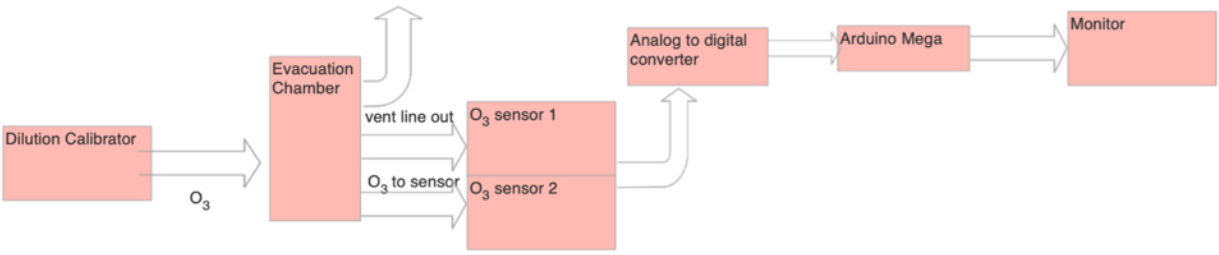

FIG. 7. Diagram of O3 calibration setup at Oklahoma Department of Environmental Quality

c. Sensor Calibration

A pair of SM50 units were taken to the Quality Assurance Lab of the Air Quality Division of the Oklahoma Department of Environmental Quality in Oklahoma City for calibration against known ozone concentrations. The purpose of the visit was to determine any offset in concentrations measured by the SM50s in a controlled environment. Both sensors were affixed to a single equalization tank using a 3 in piece of 1/2 in OD x 3 in Teflon tubing over the intake screen of the sensor (Figure 7). An outlet tube was also connected to the equalization tank to prevent excess air from being forced into the sensors. The equalization tank was connected to a dilution calibrator and ozone photometer which mixes oxygen with the ozone. When ozone reaches the sensor, the output is initially a voltage. An analog to digital converter (ADC) then converts the analog signal that is output by the sensors into a digital signal which can be sent to either an Arduino Mega or the Pixhawk. From here, it can be converted to a concentration.

The calibration started by exposing the sensor to 150 ppb of ozone, which is the maximum concentration the SM50 can accurately read. The dilution calibrator required 12 min to stabilize at the set point. Once the concentration was stabilized, 5 readings were taken at that known concentration and the reading was recorded in the Arduino monitor as well as by hand. The concentration was stepped down by 30 ppb to 120 ppb, and the process was cycle was repeated until 30 ppb was reached. The this point the step down was decreased to 15 ppb for the last experimental cycle. Finally, a blank was used as a control. A calibration curve was created from the averages of each trial by fitting a linear function to the data.

d. Challenges to SM50 Integration

One of the challenges that was faced when integrating the SM50 into the copter was how to insure proper airflow was achieved for the sensors. The SM50 sensor requires a laminar flow of air, which is difficult to achieve on a rotorcraft. Additionally, with the sensors being housed in a closed box, airflow is restricted. To combat that problem, the box was built to contain the sensors as well as a secondary motor to pump fresh air into the box with the sensor. As the sensor fans activated, the second motor would also activate and pull fresh air into the box for 30 s. The sensors would then read and average the sample taken over another 30 s, then the sequence would start again.

The other issue with integration was the timing of the fans. Since the fans from both sensor needed to both be activated at the same time. The sensor wires that were running from the fan to board were spliced to incorporate the second motor allowing it to be in a parallel sequence with the fan. This resolved the fan and airflow issue.

4. Results and Discussion

Based on the results obtained from the calibration experiment (Figure 8 and Table 1), the experimental value obtained using the sensor is much lower than the expected value. However, the measurements from the SM50 strongly correlate with the magnitude of decrease to the reference values. The coefficient of determination (R^2) for the line of best fit was 0.96. An R^2 value closer to one denotes that the experimental concentration and actual concentration are closely related to one another. The R_2 value of 0.96 means that 96% of the variation in the experimental concentration can be explained by the actual concentration. The remaining 4% remains unexplained and could be due to errors in sampling. Because there is such a strong linear correlation, this information can be used to correct the data that is obtained in the field using linear regression analysis. This is done by solving for the actual concentration and determining the offset value for the field concentration and applying this correction factor to find the actual concentration obtained in from sampling.

Finally, given the nature of the project and the time allotted to complete it, no data were collected in the field. However, significant strides in achieving a prototype platform were made, and research is still ongoing to continue with these efforts.

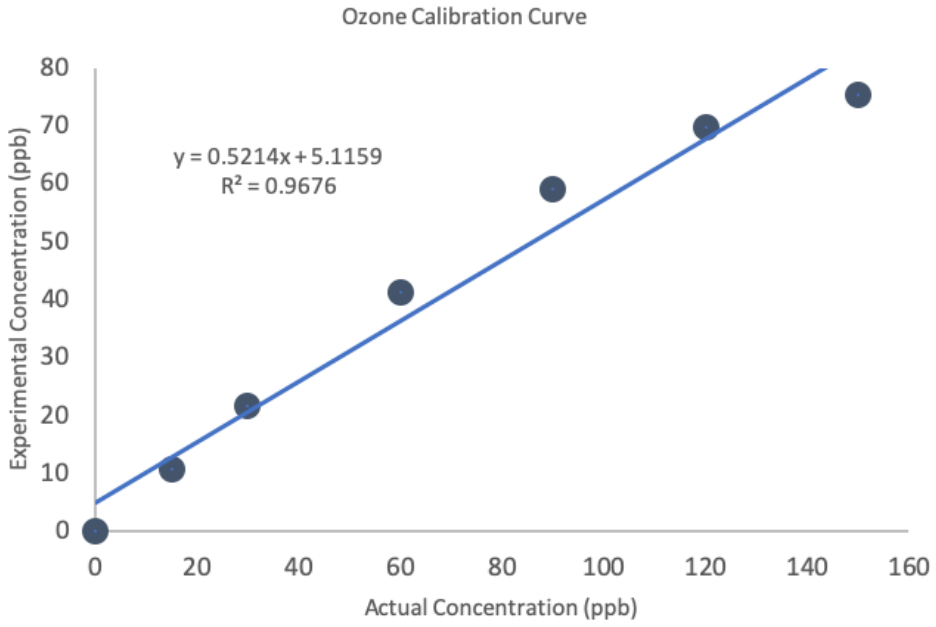

FIG. 8. QA calibration curve allows us to compensate for any discrepancies in the ozone readings obtained in the field by solving for x in the linear equation. The x axis is the known concentration output by the dilution calibrator. The Y axis is the concentration value received by the sensor.

Test #	Calibration Average (ppb)	Target (ppb)
1	0	0
2	10.85	15
3	21.728	30
4	41.408	60
5	59.0336	90
6	69.762	120
7	75.4775	150

TABLE 1. Calibration points from the Oklahoma DEQ.

5. Conclusion

This research project began with the goal to gain a better understanding of the vertical and temporal distribution of ozone in the PBL by integrating ozone sensors into a UAS. The data to be collected would add to an expansive network of satellites, ozonesondes, and ground stations already active, that collectively provide a look at ozone concentrations worldwide. Current methods leave some parts of the troposphere under-examined, leaving large gaps in the data. Though the time was limited, we were able to characterize the sensors, develop code for the sensors to communicate with the CopterSonde autopilot system, and calibrate the sensors to make any corrections in data obtained in the field. One of the most challenging components of this project was to integrate the sensors into CopterSonde 3. The SM50 sensor first had to be integrated with an analog to digital converter, Pixhawk autopilot, a separate fan motor, and a power source. Having these extra components made integration into CS3 more difficult, as code had to be written for the additions to the sensor package. The housing for the sensor package also had to be created and the sensors, along with the extra components, had to be placed into the housing and secured. With the sensor package integrated and tested successfully, we are able to test fly the copter in the field up to 120 m. Currently, a CO_2 sensor is being used to collect data.

Using the framework for integration described in this work, a clear path for integrating chemistry payloads into UAS has been established. Future work can now be done with the newly integrated ozone sensors and the team can begin to incorporate carbon dioxide, ozone, and aerosol sensors into the copters into a full chemistry package.

Acknowledgments. I would like to extend my gratitude to my mentors Dr. Liz Pillar-Little, Brian Greene, and Tyler Bell, for their support and encouragement. I would like to give a special thanks to the Center for Autonomous Sensing and Sampling (CASS) engineers, Gus Azevedo and Tony Segales for helping make the science and technology work together and to the Oklahoma Department of Environmental Quality Air Quality Division for allowing use of their facilities for sensor calibration. This material is based upon work supported by the National Science Foundation under Grant No. AGS-1560419.

References

Baird, C., and M. Cann, 2012: *Environmental Chemistry*. 5th ed., W.H. Freeman and Company.

Environmental Protection Agency, 2019a: EPA air quality monitors map. https://epa.maps.arcgis.com/apps/webappviewer/index.html?id=5f239fd3e72f424f98ef3d5def547eb5&extent=-146.2334,13.1913,-46.3896,56.5319.

Environmental Protection Agency, 2019b: Health effects of ozone pollution. https://www.epa.gov/ground-level-ozone-pollution/health-effects-ozone-pollution.

Felzer, B. S., T. Cronin, J. M. Reilly, J. M. Melillo, and X. Wang, 2007: Impacts of ozone on trees and crops. *Comptes Rendus Geoscience*, **339 (11-12)**, 784–798.

Manahan, S., 2010: *Environmental chemistry*. Ninth ed., CRC press.

National Aeronautics and Space Administration, 2019: Aura satellite OMI instrument. https://aura.gsfc.nasa.gov/omi.html.

National Oceanic and Atmospheric Administration, 2018: Ozonesonde sites. https://www.esrl.noaa.gov/gmd/ozwv/ozsondes/.

Stull, R., 1988: *An Introduction to Boundary Layer Meteorology*. 9th ed., Dordrecht.

Williams, D. E., 1999: Semiconducting oxides as gas-sensitive resistors. *Sensors and Actuators B: Chemical*, **57 (1-3)**, 1–16.

Zielke, B. S., 2011: A procedure for obtaining high-density in-situ measurements of ozone concentration within the planetary boundary layer. M.S. thesis, University of Oklahoma.